Magazine of Civil Engineering

ISSN 2712-8172

journal homepage: http://engstroy.spbstu.ru/

Research article

UDC 624.154

DOI: 10.34910/MCE.116.6

Temperature effects on the design parameters of a geothermal pile

***W. Arairo*[1] ✉, *F. Masrouri*[2], *A. Abdallah*[2], *S. Rosin-Paumier*[2], *O. Sraj*[3], *M. Khatib*[4]**

[1] *University of Balamand, Kurah, Lebanon*

[2] *University of Lorraine, Vandoeuvre-lès-Nancy, France*

[3] *Advanced Construction Technology Services, Jeddah, Saudi Arabia*

[4] *ISSEA-Cnam Lebanon, Beirut, Lebanon*

✉ *wahib.arairo@balamand.edu.lb*

Keywords: geostructures, pressuremeter, heat transfer, temperature, conductivity, finite element method

Abstract. In geotechnical engineering, geostructures with thermo-active functions establish direct thermal exchange between the ground and buildings. They can transfer energy from or into the ground to heat or cool a building. However, adapting foundation piles, completely or in part, to produce energy piles results in heat exchange with the soil, which changes the temperature of the soil and could thereby and affects the geotechnical properties and load bearing capacity of the geostructure. Most calculations of the bearing capacities of deep foundations conducted in France are currently based on in-situ testing results using a pressuremeter. Using finite element method to model the pressuremetric behaviour of a compacted soil subjected to thermo-mechanical variations is the main motivation for this work. In this study, several pressuremeter tests were conducted on a compacted illitic soil in a laboratory tank at temperatures between 1° and 40°C. The impact of temperature variation on the limit pressure (Pl), the creep pressure (Pf) and the Ménard pressuremeter modulus (EM) were determined. The results showed a significant decrease for both limit pressure (Pl) and creep pressure (Pf) with the increase of temperature. Numerical simulations of these tests were used to calibrate a bilinear constitutive model, taking into account temperature effects on soil compressibility within a coupled thermo-mechanical framework. Thereafter, a case study of a heat exchanger pile was simulated using the proposed approach.

Acknowledge: This study was part of the GECKO research program funded by ANR.

Citation: Arairo, W., Masrouri, F., Abdallah, A., Rosin-Paumier, S., Sraj, O., Khatib, M. Temperature effects on the design parameters of a geothermal pile. Magazine of Civil Engineering. 2022. 116(8). Article no. 11606. DOI: 10.34910/MCE.116.6

1. Introduction

Geothermal energy is considered as an energy source, which has many advantages over than the conventional energy sources (concerning cost, reliability and environmental). Thermally active structures such as diaphragm walls, piles, tunnel linings, and basement walls present a promising and sustainable way for buildings heating and cooling as cited by Fromentin et al. [1], Laloui et al. [2] and Brandl [3]. The functioning of thermo-active geostructures are based on variations of the surrounding soil temperature (about 12 °C) over a range from 4 to 30 °C as discussed by Peron et al. [4]. To design heat exchanger systems, the coupled behavior between temperature variations and induced stress/strain must be taken into consideration as recommended by McCartney et al. [5], which may affect long-term performance of geostructures.

The objective of this work is to expand the understanding and measuring the impact of temperature variation on pressuremeter parameters, the pressuremetric response of soil under coupled thermal and mechanical loads to help in establishing a more effective geotechnical design criteria.

In this study, the foundation piles were considered as deep ones, and transferred the loads to depth. These foundations piles work through a combination of two phenomena's: tip resistance and lateral skin friction along the length of the pile. Several experimental investigations on the effect of temperature on soil behaviour have shown that a variation in temperature affects soil mechanical parameters (cohesion, elastic modulus, friction angle, etc.).

Modaressi and Laloui [6] summarised two major effects of heating on clays: the first one consider a thermal reversible dilation in the case of over-consolidated soils, while the second discuss an irreversible contraction in the case of a small over-consolidation ratio.

Similar results have been obtained by Burghignoli et al. [7] and later by Cekerevac and Laloui [8] for different clayey soils containing different ratios of kaolinite, illite, smectite and chlorite. For instance, these experimental results show that soil can undertake irreversible deformation when subjected to a temperature increase under a constant mechanical load equivalent to or slightly less than the preconsolidation stress.

In recent years, efforts have been made to optimise the energy performance of thermo-active geostructures. For example, in-situ tests were performed by Brandl [9], Bourne-Webb et al. [10] and Amatya et al. [11].

Several methods have been developed for determining the stress-strain response of vertically loaded piles. Two different approaches have been widely used, the finite difference model, and the finite element approach with two-dimensional elements defining the soil-pile interface.

In the finite difference approach, the pile is divided into rigid block connected by springs simulating the stiffness of the pile. Each element is subjected to an elastoplastic interaction with the soil interface. The load-transfer curves describe the relation between the shaft friction and the pile displacements, along with the relation between the pressure at the tip of the pile and the pile displacement. To introduce the effect of cyclic temperature variation, several authors like Knellwolf et al. [12], Bourne-Webb et al. [13] have added an unloading term to the load-transfer curve to characterise the reversible behaviour of the soil-pile interaction due to thermal cyclic loading. However, the soil and soil-pile interface properties remain constant with temperature.

In another approach, different constitutive soil models have been developed to introduce the effect of the temperature on the yield surface by Graham et al. [14], Cekervac and Laloui [8]. The soil-pile interface can be defined by zero thickness elements as discussed by several authors such as Goodman et al. [15], De Gennaro and Frank [16], Said [17] or thin layer elements as cited by Desai and Faruque [18].

Currently, the use of finite element methods in engineering to assess thermo-hydro-mechanical behaviour remains limited because the method is time consuming and constitutive models (for soil and soil-pile interface) frequently require numerous parameters that are difficult to access. Therefore, there is a need to develop efficient soil models that involve a few accessible parameters and are still able to reproduce correctly the soil behaviour. The simplest methods of simulating the soil-pile behaviour remain the ones based on the use of load-transfer curves.

Several load-transfer curves are available in the literature of Randolph and Wroth [19], Frank and Zhao [20] also Armaleh and Desai [21]. Load-transfer curves are defined using the pressuremeter modulus, the limit pressure, the pile diameter and the piling method. The pressuremeter is a standard in-situ test for soils and rocks providing information on strength and stiffness parameters and were mentioned by AFNOR [22] and ASTM D 4719 [23]. It provides a means of designing piles that meet both failure and deformation criteria.

The design method based on pressuremeter parameters proposed by Knellwolf et al. [12] is based on the following considerations: (1) the main component of the displacement is the axial displacement of the pile. The radial displacements of the pile are neglected, (2) the Young's modulus and coefficient of thermal expansion of the pile remain constant and independent of the temperature change, (3) the soil and soil-pile interface properties are not affected by the temperature.

In this paper, the conformity of Knellwolf hypotheses is interpreted based on the experimental results described later and the current state of knowledge of the thermo-mechanical coupled behavior of soils. The first hypothesis, which considering only the axial strain of the pile induced by temperature, matches with the results of a study by Olgun et al. [24]. Despite the fact that several experimental studies have shown that thermal cycles induces volume changes as described by Abuel-Naga et al. [25, 26] the axial displacement remains the major component.

The experimental results of Shoukry et al. [27] do not match with the second hypotheses of Knellwolf et al. [12], Amatya et al. [11], and Bourne-Webb et al. [13], as they show that the concrete elastic modulus is affected by the temperature change.

With respect to assumption no. 3, the experimental results of the pressuremetric tests conducted under controlled temperatures developed here and several researches were achieved by numerous authors like Graham et al. [14], Cekerevac and Laloui [8], Abuel-Naga et al. [28–30], show that soil-engineering properties are temperature-dependent. Therefore, it is highly probable that the temperature influences the soil-structure interface behavior. The lateral confining effective stress on the soil-pile interface could be misestimated leading to a miscalculation of the pile shaft resistance under thermal cyclic load of heating/cooling. Further investigation is required to confirm this point.

In this study, the soil used, the experimental device and the mini-pressuremeter method are described. Then, the thermal transfer associated with the heating and cooling phases before the pressuremeter tests is numerically simulated. A finite element model based on a bilinear constitutive law is used to simulate the mini-pressuremeter tests. In this model, the soil compressibility is temperature-dependent in a coupled thermo-mechanical framework. Afterwards, the experimental and numerical results are presented and discussed, focusing mainly on the thermal induced effect on the geotechnical design parameters of energy piles. A model problem of geothermal pile is developed using the proposed model with finite element method, in axisymmetric stationary conditions. Unlike other proposed models based on pressuremeter parameters proposed by Knellwolf et al. [12], Amatya et al. [11], and Bourne-Webb et al. [13], the soil-pile interaction properties depend on the temperature variation. Finally, the effect of cyclic temperature variation on the mechanical behaviour of the pile is concluded.

2. Methods

To investigate the effect of thermal loading on the pressuremeter parameters of a compacted soil, a small-scale tank was developed in the laboratory, and mini-pressuremeter tests were performed on the compacted soil.

Ever since the finite element was described early by Turner et al. [32] and applied to the analysis of elasticity problems, a huge number of methodologies for modeling the variation formulation of certain other field problems such as seepage, heat conduction, or consolidation that are of interest in soil mechanics have been established.

The obtained experimental results were compared with the same model using a finite element software. The objective of this comparison is to validate the experimental results and highlight the effectiveness of the proposed model.

2.1. Material and experimental device

Arginotech©, an illitic soil from eastern Germany was studied. It contains 76 % illite, 10 % kaolinite, 12 % calcite and traces of quartz and feldspar. Illite shows temperature-dependent behaviour as discussed by Tanaka et al. [33]. It is a non-swelling clay present in variable proportions in soils due to mineral illitisation as expressed by Lynch [34].

The grain size distribution of the soil was determined using a laser granulometer device (Figure 1b). Almost 85 % of the particles of the considered material were clay particles, and 15 % were silt particles. The Atterberg limits were determined according to AFNOR [35] and the results are as follows: liquid limit (LL = 65 %), plastic limit (PL = 34 %), and plasticity index (PI = 31 %). The standard Proctor curve obtained for the illitic soil mentioned in AFNOR [22] defines an optimum water content (w/c) equal to 31.26 % and a maximum dry density of 1.42 mg/m^3 (Figure 1a). The soil is considered as class A3 according to the French soil classification standard [36] and as a fat clay, MH, according to the Unified Soil Classification System ASTM [37].

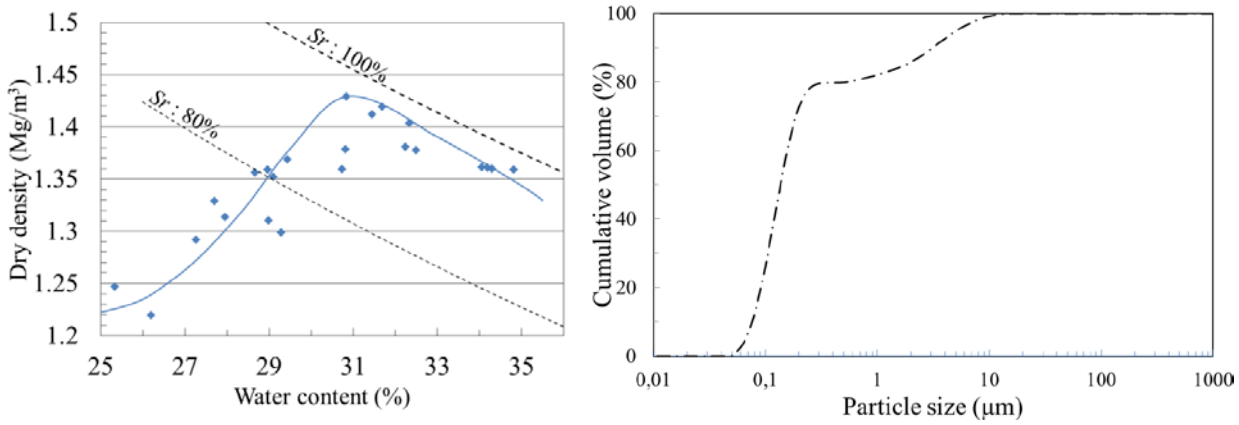

a) Compaction curve of the illitic material. Sr: The degree of saturation.

b) Particle size distribution of the illitic material.

Figure 1. Characteristic of the studied illitic soil.

The thermal conductivity of the material studied was measured with the KD2Pro© thermal properties analyser equipped with an SH1 sensor. The suction of the studied material was measured with a WP4C water potential meter. The samples were prepared at the same dry density and the same water content as the compacted soil in the tank. In such conditions, the thermal conductivity λ reached 0.81; 0.83; and 0.88 W.m/K at 1°, 20° and 40 °C, respectively. The measured suction reached 220 and 380 kPa at 20° and 40 °C, respectively.

2.2. Sample preparation and compaction in the small-scale model

The small-scale model consisted of a stainless steel cylindrical container with a height of 800 mm and a diameter of 600 mm. The soil was compacted using a dynamic compactor and a metallic plate to distribute uniformly the compaction energy over the whole surface of the soil layers, each 70 mm thick.

Thermal sensors (7 sensors) were introduced within the container to monitor temperature inside the compacted soil during the imposed temperature variations.

A Vulcatherm® thermosregulator was connected to stainless steel tubes welded to the outer contour of the soil cylinder. A solution of ethylene glycol and water was circulated in the tubes to impose the thermal variations (1, 20 or 40 °C). Insulating sleeves were placed on the steel tubes to reduce heat transfer with the surrounding atmosphere (Figure 2). Finally, a box made of 40 mm thick extruded polystyrene plates, was used to insulate the whole assembly.

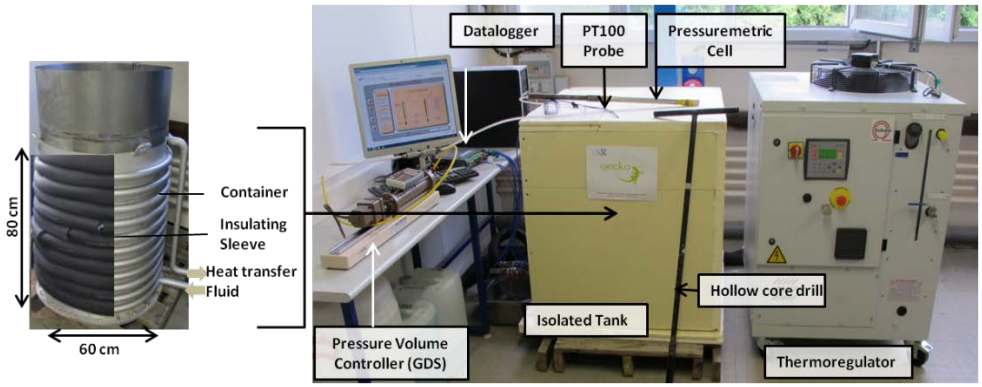

Figure 2. Experimental device designed to carry out temperature controlled mini-pressuremetric tests.

In this study, two tanks were prepared with the illitic material, compacted at the Proctor optimum water content of 31.3 % and a dry density of 1.29 mg/m^3, corresponding to 90 % of the Proctor maximum dry density. An initial temperature of $Ti_1 = Ti_2 = 20$ °C was applied to the soil for 75 hours before the thermal loading. Then, tank 1 was heated to $Tf_1 = 40$ °C for 75 h, and tank 2 was cooled to $Tf_2 = 1$ °C for 75 h.

2.3. Mini-pressuremeter tests

The test consists of introducing a cylindrical probe with a flexible membrane, which can expand radially into a drilled core to the desired testing depth. Pressure is applied to the walls of the borehole by

the probe, and the soil deformation volume is measured. Three parameters are used to mention the pressuremeter E_M, p_L and p_f.

Before each mini-pressuremeter test, a 630 mm core was drilled with a diameter equal to the mini-pressuremeter probe. The cored material characterisitcs (i.e. the water content and the dry density) were measured each 25 mm in height. All water contents range between 29.7 % and 32.6 %, while the dry densities ranged from 1.23 to 1.40 mg/m^3 (Fig. 3). These distributions as a function of depth showed acceptable deviations (+/-3%) in comparison with the target values and validated the suitable overall homogeneity of the sample. The mini-pressuremeter tests were carried out with an APAGEO® mini-pressuremeter probe. The pressuremeter test consisted of applying increasing incremental pressure rate of 25 kPa per minute as recommended by AFNOR [22], and ASTM D4719 [23]. The equilibrium volume of the probe was measured for each pressure increment and the volume as function of the applied pressure were plotted with a maximum reached volume of the probe of 140.000 mm^3.

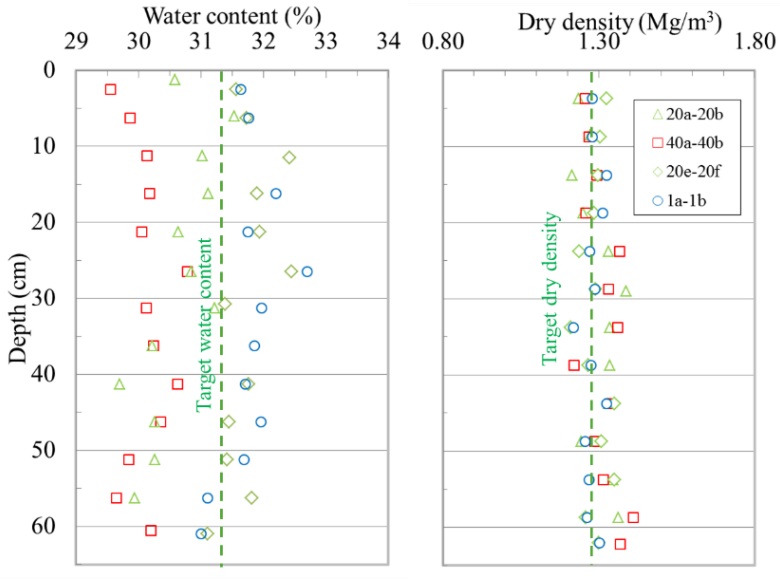

(a) Water content distribution over depth **(b) dry density distribution over depth**

Figure 3. Water content and dry density distribution in both tanks.

In the tank 1, two mini-pressuremeter tests (Fig. 4) were carried out at an initial temperature of Ti_1 = 20 °C (20a, 20b) and two others at Tf_1 = 40 °C (40a, 40b). In the second tank, two mini-pressuremeter tests were performed at Ti_2 = 20 °C (20e, 20f) and two others at Tf_2 = 1 °C (1a, 1b).

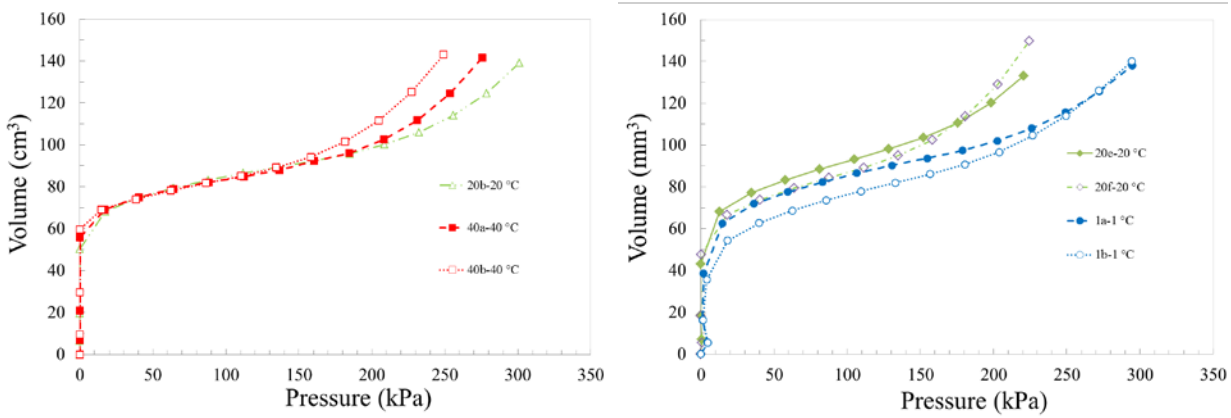

(a) Pressuremeter curves at 20 and 40 °C (data from Tank1)

(b) Pressuremeter curves at 20 and 1 °C (data from Tank2)

Figure 4. Pressuremeter curves.

To control the thermal diffusion in the studied illitic soil, seven thermal sensors were introduced at different positions in the tank: D1 = 50 mm, D2 = 150 mm, D3 = 300 mm from the lateral boundary (Fig. 5). The temperature variation was recorded throughout the test.

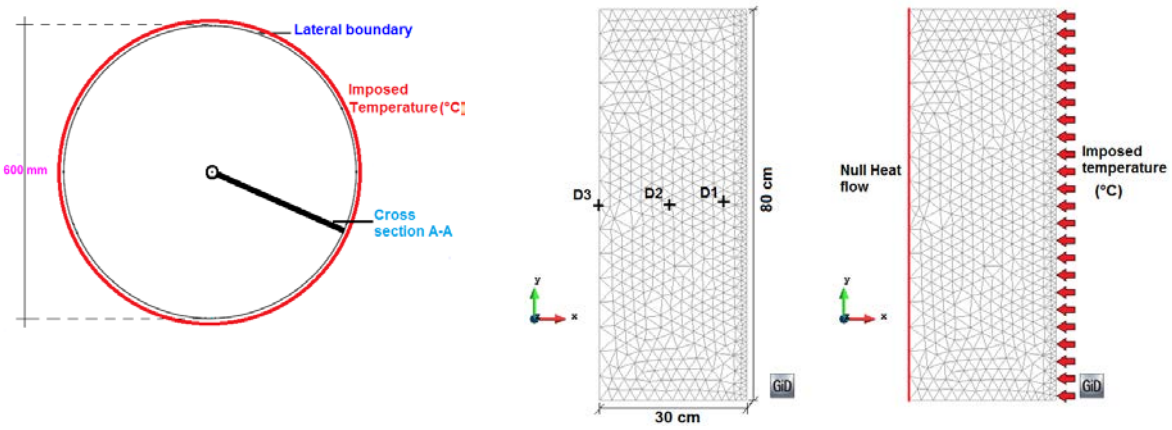

(a) Plan view of the cylindrical tank **(b) Geometry and mesh** **(c) boundary conditions of meshed cylinder**

Figure 5. Simulation the heat propagated in the cylindrical tank.

During the heating phase, a temperature of 41 °C was applied; the referred 40 °C temperature was reached after approximately 22 hours, 40 hours, and 47 hours of heating at 50 mm, 150 mm and 300 mm from the heat source respectively. For the cooling phase, a temperature of 1 °C was applied. At steady state, the temperature was approximately 2 °C. This temperature was reached after 39 hours, 67 hours and 75 hours for points 50 mm, 150 mm and 300 mm from the lateral boundary respectively.

2.4. Pressuremeter parameters of the soil submitted to thermal variations

The first test at 20 °C has failed due to membrane leakage. The results of the other tests carried out at different constant temperatures are presented in Fig. 4(a). The pressuremeter curve consists of three parts. First, the probe volume increases to reach contact with the wall of the borehole. Than a linear increase of the volume with increasing pressure is observed, in this part, the pressuremeter modulus E_M (deduced from the slope of the pressuremeter curve) is calculated, and finally, large displacements take place and the soil reaches its plastic domaine. The creep pressure, p_f, the boundary between the second and third steps of the test, is determined on the creep pressuremeter curve (standard NF P94-110-1, AFNOR [22]). The limit pressure is the extrapolated pressure at which the injected volume reaches twice the initial volume of the hole. The pressuremeter parameters E_M, p_L and p_f for each test are summarized in Table 1

The results showed a negligible effect of temperature variation on E_M parameter, while the p_f and p_L pressures increased with cooling (decrease of temperature). The material undergoes plasticity earlier when heated since the plastic deformations started earlier for the tests at 40 °C, than at 20 °C and 1 °C, approving a reduction of the elastic zone.

Table 1. Experimental results of different pressuremeter tests carried out at different constant temperatures tank1 (20 -40-20 °C) and Tank 2 (20-1-20 °C).

Test	Test number	Temperature (°C)	E_M (MPa)	p_f (MPa)	P_L (MPa)	E_M / p_L
Tank1	20b	20	3.54	0.198	0.357	9.916
	40a	40	3.52	0.163	0.317	11.104
	40b	40	2.94	0.162	0.283	10.389
Tank2	20e	20	2.28	0.14	0.316	7.215
	20f	20	2.29	0.143	0.258	8.876
	1a	1	2.85	0.207	0.365	7.808
	1b	1	2.49	0.19	0.357	6.974

The drop of the studied parameters could be justified by the thermal softening due to increasing temperature. Similar results concerning the decrease of the yield limit with heating were also detected in triaxial tests for other types of materials achieved by Lingnau et al. [38], Marques et al. [39], Uchaipichat and Khalili [40].

2.5. Numerical simulation

Two different numerical simulations are presented in this section. The first simulation concerns thermal transfer during the heating and cooling phases. The second simulation focuses on the mini-pressuremeter test parameters under controlled temperatures. The numerical calculations were carried out using the Code_Bright finite element code Olivella et al. [41]. For each simulation, the numerical strategy is detailed first, describing the different steps of the modelling. Then the numerical setup is presented, with the considered mesh, also initial and boundary conditions. Finally, the results are interpreted.

2.5.1. Thermal transfer approach

Thermal transfer between the lateral boundary and the soil generated a variation in the tank temperature profile.

For soils, the conduction is considered as the primary heat transfer mode especially in clayey soils where the hydraulic conductivity is very small. The main thermos-physical properties that control the heat flow by conduction are D, λ, C_v. The relation between the three properties is given as follows:

$$D = \frac{\lambda}{C_v}. \tag{1}$$

Many studies have considered that the total heat capacity of a given soil is the resultant of the heat capacities of the soil components to estimate C_v De Vries and Afgan [42]. These thermal properties depends on the mineral composition of soil and on its porosity n as follows:

$$C_v = (1-n)\rho_{cs}c_{T_s} + n\rho_{cw}c_{T_w}. \tag{2}$$

The conductive heat flow i_c is governed by Fourier's law:

$$i_c = -\lambda \nabla T. \tag{3}$$

Different formulations for the thermal conductivity λ have been proposed in the literature. This parameter has been related to soil properties such as mineralogical composition, dry density, pore fluid, degree of saturation, water content, temperature, and geometrical arrangement of soil particles following the recommendations of Brandon and Mitchell [43, 44].

It is reasonable to assume that the thermal conductivity of the soil remains constant, since the experimental test conditions requiring complete isolation of the tank and the small variation of thermal conductivity of the soil within the studied ranges of temperature.

To validate the main assumptions concerning the heat transfer including (1) consideration of conductive heat transfer only, (2) the use of a constant thermal conductivity, and (3) consideration of the medium as homogeneous with respect to apparent properties without taking into account the contribution of each phase, a basic numerical study was performed.

Owing to the symmetry of the problem (i.e., load and geometry axial symmetry of the tank), the problem can be reduced to a two-dimensional axisymmetric condition with respect to the vertical axis (oy). The soil mass was discretised into an unstructured mesh of triangular finite elements. A null flux was imposed on the symmetry axis. Only the temperature was fixed on the outer border; no mechanical load was taken into account. Initially, the temperature of the soil was homogeneous and constant (Ti = 20 °C). The thermal loads were applied continuously by imposing a constant temperature on the outer lateral boundary. The parameters used in the simulation are summarised in Table 2. It should be noted that in the studied case, only the apparent conductivity and apparent specific heat were considered (Table 2). Other heat transfer processes (i.e., convection and radiation) have been neglected.

Table 2. Parameters used in the numerical simulation of heat transfer.

C_v, (J/kg.K)	λ (W.m/K)
1796	0.924

In this section, the main results of heat propagation simulation are presented. The calculation was performed using the finite element code Code_Bright. Initially, the temperature was uniform (Ti = 20 °C). Two simulations were performed. Following the experimental conditions, for the first simulation, the imposed temperature at the lateral outside boundary was 41 °C for 75 h. For the second simulation, the lateral outside imposed temperature was 1 °C for 75 h.

The time variation of the temperature, plotted in Figure 6, shows the heat transfer phenomenon at different positions from the heat source: D1 = 50 mm; D2 = 150 mm; D3 = 300 mm (see Fig. 5 for more details of the geometry and the position of heat sensors). According to Fig. 6, the numerical model, with the parameters given in Table 2, is able to reproduce the heat propagation correctly at different distances from the heat source. A slightly higher value for heat conductivity than the experimentally measured value was used to superimpose the experimental and numerical results. However, the difference remains in the range of accuracy of the KD2Pro© thermal properties analyzer used (± 10 %), and both curves (the numerical and the experimental one) converge to the same steady state limit.

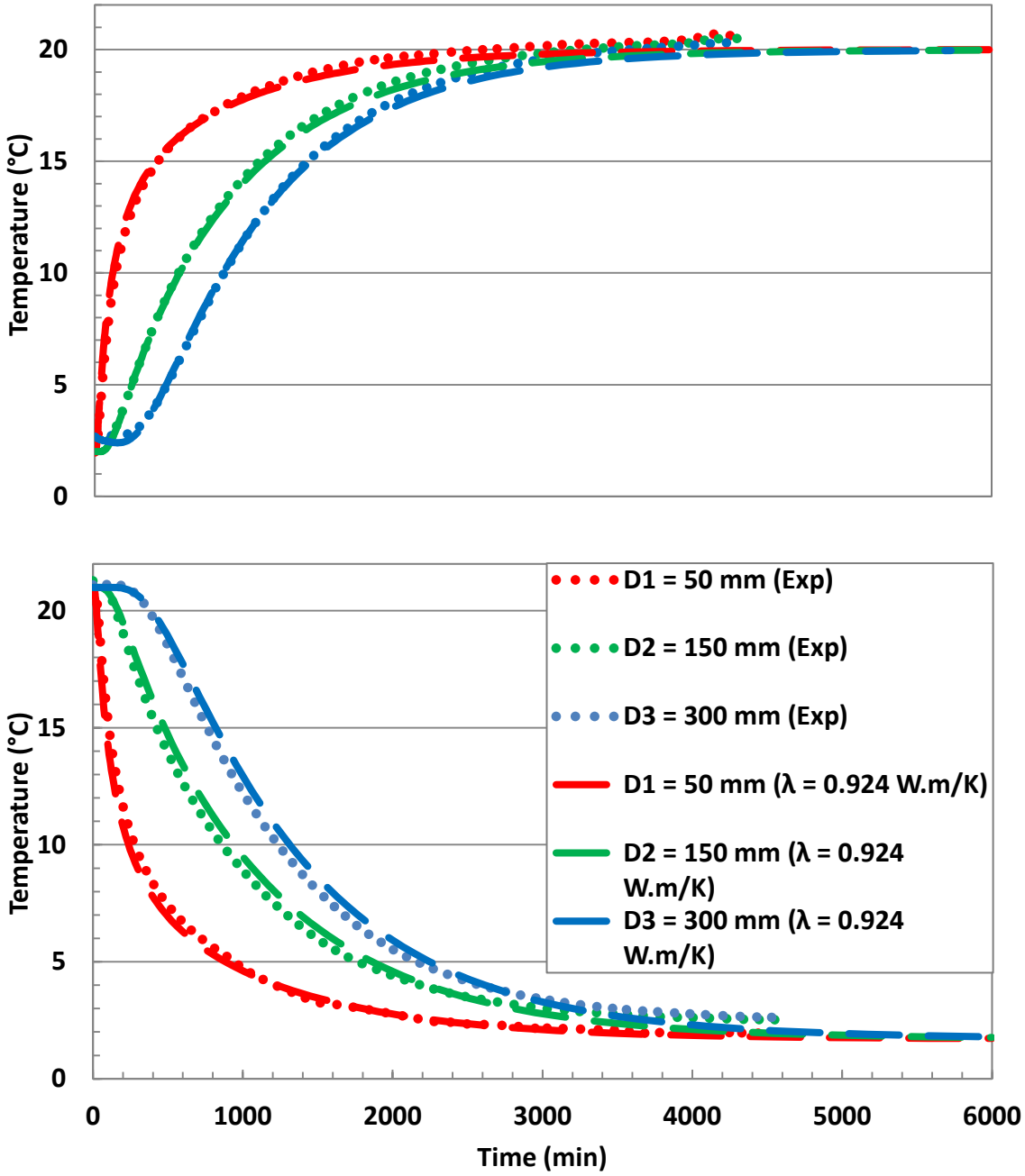

Figure 6. Time evolution of the temperature at different distances from the imposed heat temperature ((a): T = 40 °C (b): T = 1 °C) on the outer lateral boundary starting from initial temperature (T = 20 °C).

2.5.2. Simulation of mini-pressuremeter tests at different imposed temperatures

The mini-pressuremeter tests performed in the compacted soil at various temperatures were modelled using a bilinear elastoplastic model. In this section, the model parameters are presented, and the effect of temperature on the pressuremeter parameters $\left(E_M,\ p_L,\ p_f\right)$ is discussed.

Bilinear model simulating the pressuremeter results

Soils are mainly frictional granular media, with mechanical behaviour that is well described within the framework of elasto-plasticity theory. The model used here to characterise the mechanical behaviour of the soil is a basic bilinear model. The main equations and parameters used are presented in the following text.

The bilinear model involves four parameters: $E_0,\ E_c,\ \nu,$ and ε_{vlimit}.

The limit between the initial $\left(E_0\right)$ and final $\left(E_c\right)$ slope is given by the definition of the limit strain ε_{vlimit}. The stress-strain relation describing the mechanical behaviour is given by the following equations:

$$\text{If } \varepsilon < \varepsilon_{\nu\ limit} \rightarrow \sigma = E_0\varepsilon$$

$$\text{If } \varepsilon > \varepsilon_{\nu\ limit} \rightarrow \sigma = E_0\varepsilon_{\nu\ limit} + E_c\left(\varepsilon - \varepsilon_{\nu\ limit}\right). \tag{4}$$

Fig. 7 shows the stress-strain relation with the different parameters involved to characterise the mechanical behaviour.

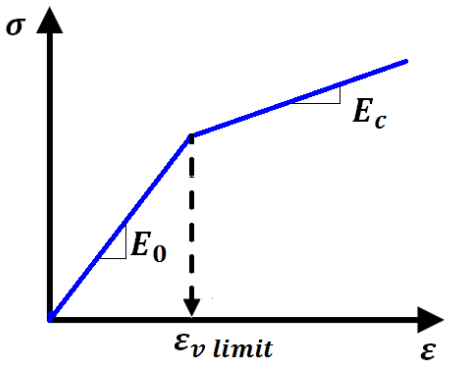

Figure 7. Bilinear model defining the stress-strain relation.

Geometry, mesh and boundary conditions for the mini-pressuremeter thermally controlled test

The geometry of the tank, with its adopted mesh was presented in Fig. 8. The calculation was performed in two steps: the thermal loading phase, involving the application of a constant temperature throughout the soil and; the execution of the mini-pressuremeter test at 150 mm from the boundary.

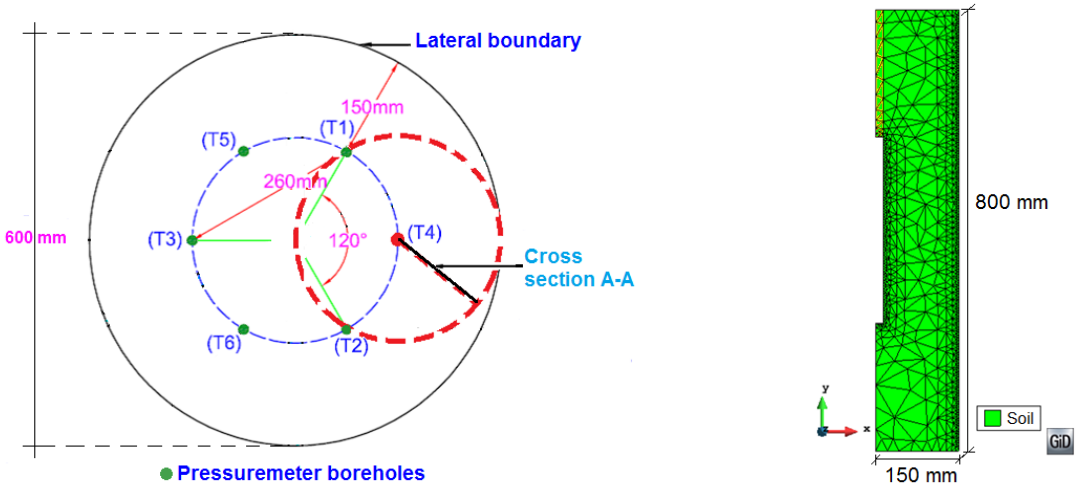

(a) geometry of the tank in plan view **(b) meshed axisymmetric vertical view**

Figure 8. Numerical simulation view.

The boundary conditions for the two calculation steps are given in Fig. 9. Zero horizontal displacement conditions were applied to the outer lateral border, and a total fixity condition was imposed on the lower limit. The first part of the mini-pressuremeter test, which corresponds to the probe inflation to contact the wall of the hole, was not simulated because it is not necessary for determining the pressuremeter parameters (i.e., the pressuremeter modulus and the creep and limit pressures). Only the pseudo-elastic and plastic parts of the pressuremeter curves are considered (zones 2 and 3 in Fig. 10).

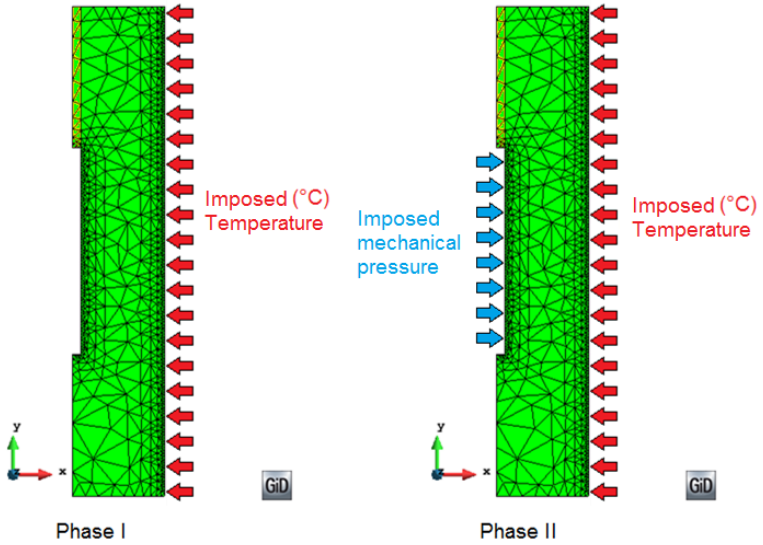

(I) Heat imposed phase (II) pressuremeter under constant temperature test phase

Figure 9. Boundary conditions for the two calculation steps.

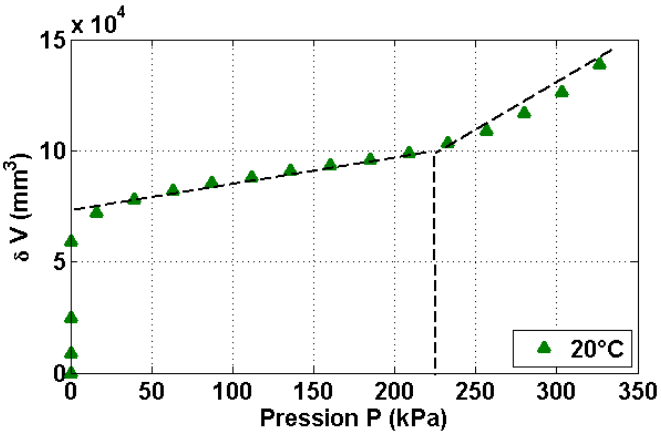

Figure 10. Determination of model parameters (E_0, E_c, ε_{vlimit}) according to temperature variation with initial and final slopes and strain limit value.

According to the French design standard for deep foundations, Young's modulus can be related to the pressuremeter modulus by using α. The relation between E_0 and E_M is given by the following equation:

$$E_0 = \frac{(1+\nu)(1-2\nu)}{\alpha(1-\nu)} E_M . \tag{5}$$

Ménard [45] was estimated α for clayey soils from the E_M / p_L ratio and was found that α = 0.5. To include the effect of temperature variation on the mechanical behaviour, the model parameters were determined, as functions of temperature, as follows:

E_0 was calculated, based on the pressuremeter modulus E_M (equation 5), E_c was fitted to the corresponding experimental test results, and ε_{vlimit} was calibrated according to the experimental results.

ν = 0.3 was considered constant.

For each simulation, the values of the mechanical parameters are summarised in Table 3. These parameters were defined according to the average value of the pressuremeter modulus for the two tests at the same temperature. It should be noted that thermal parameters were kept unchanged and identical to those given in Table 2.

Table 3. Mechanical parameters used for the simulation of pressuremeter tests for different temperatures.

Tanks	Temp (°C)	E_M (MPa)	E_0 (MPa)	ε_{vlimit}	ν	E_c (MPa)
Tank1	20	3.54	5.27	0.00335	0.3	0.3
	40	3.231	4.8	0.00218		
Tank2	20	2.285	3.39	0.003	0.3	0.3
	1	2.666	3.96	0.0035		

The parameter's calibration shows that E_0 and ε_{vlimit} are temperature dependent, while E_c remains constant (Fig. 10).

3. Results and Discussions

3.1. Pressuremeter parameters of the soil submitted to thermal variations

The main experimentally results of mini-pressuremeter test simulations under controlled temperature are presented in this section. The volume variations versus the applied pressure are shown for the two tanks in Fig. 11. The proposed bilinear model was calibrated by comparing experimental data to analytical simulations. The model is able to reproduce the volumetric variations against the applied pressure at a constant temperature correctly. Moreover, these curves show that the pseudo-elastic behaviour can be considered slightly sensitive to temperature. The pressuremeter modulus decreases slightly when the temperature increases. However, the effect of temperature is more significant on the two other parameters; creep pressure pf and the limit pressure p_L.

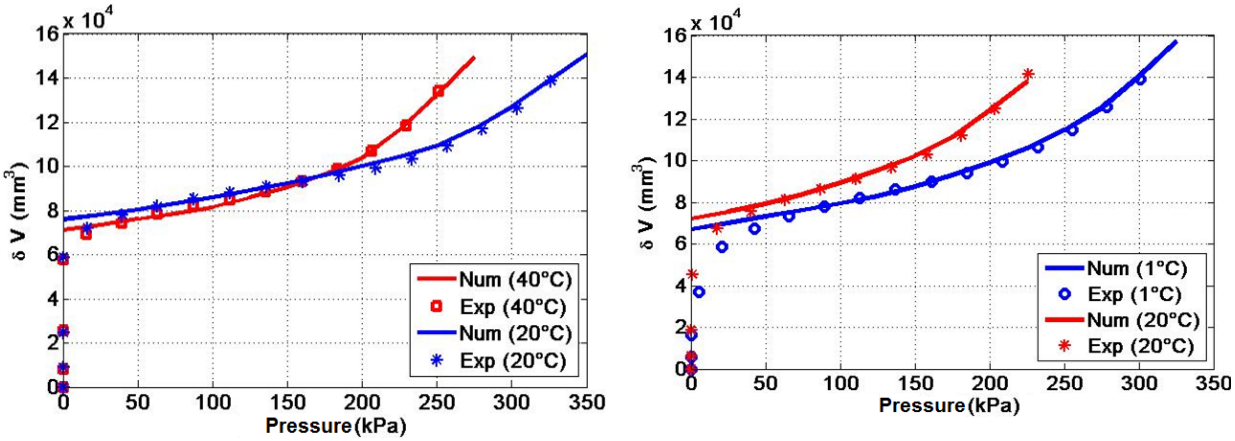

(a) Ti_1 = 20°C and Tf_1 = 40 °C **(b) Ti_2 = 20 °C and Tf_2 = 1 °C**

Figure 11. Numerical and experimental variation of volumetric deformation against applied pressure under variable Ti and Tf.

The creep pressure decreased significantly with the increase in temperature. In the numerical model, this resulted in a decrease of the limit deformation ε_{vlimit}. This means that the soil exhibited a thermal softening. Qualitatively, this result represents a transition to a more ductile behavior. These results match those obtained by Hueckel et al. [46], Laloui [47], who found that the yield surface decreased with increasing temperature.

As a first approach, a linear relation between the temperature T and the ε_{vlimit} is considered. According to the experimental results, the following relation can be proposed for the material studied (Fig. 12):

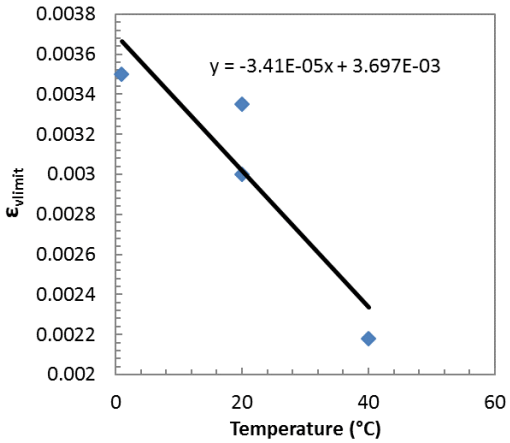

Figure 12. Proposed linear variation of ε_{vlimit} against temperature.

$$\varepsilon_{vlimit} = -3.41e^{-5}T + 3.697e^{-3} \quad (6)$$

This relationship has been introduced into the finite element code to take into account the effect of temperature on mechanical behavior for a better simulation of the interaction between the energy pile and the soil. Other formulations involving cyclic thermal variation are to be investigated.

3.2. Simulation of the energy pile behaviour using simplified model

A concrete pile of 1 m diameter and 20 m length was studied. A parametric study has been performed to ensure adiabatic boundary conditions in order to select the soil mass boundary dimension. The horizontal radius was set to 50 m from the pile lateral surface and the height of the soil mass to 60 m. The complete domain was simulated using a 2D axisymmetric model. Stationary analyses were executed to determine the magnitude of soil strength in response to thermal pile loading.

Fig. 13 shows the dimensions of the simulated domain and the pile. The temperature was assumed to be constant throughout the pile length, based on the results reported by Suryatriyastuti et al. [48]. An analysis of this uncoupled thermo-mechanical model was carried out using finite element code (Code_Bright). First, the mechanical load due to the weight of the building was considered; then, the thermal load was applied. The pile was maintained in rigid contact with the surrounding soil. The surrounding soil was modelled with bilinear conditions and the parameters were temperature-dependent.

The thermal loading is applied as stationary condition in the pile; a fixed condition is assigned on the bottom boundary; a null head flow condition is imposed on the lateral boundary. The thermal loads were applied continuously over a one-year period and homogeneously over the whole pile section with the values summarised in Table 4. Table 5 summarises the thermo-mechanical properties of the materials used in this case study.

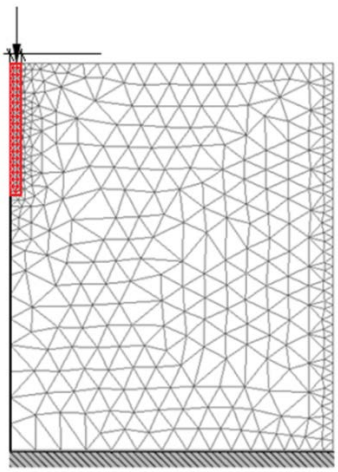

Figure 13. Mesh and geometry of the studied heat exchanger pile.

Table 4. Applied temperature in the heat-exchanger pile.

Calculation step	Pile Temperature (°C)	Period (days)
1	16	30
2	32	180
3	2	180

The variation of the applied temperature is shown in Figure . The ground temperature was initially generated taking into consideration its variation with depth between 12° and 17 °C. This temperature was kept constant throughout the test, since the study is limited to stationary analysis. After that, the top of the pile was loaded with up to 270 kPa corresponding to the mechanical load applied by the upper structure. The system was then subjected to two different seasonal thermo-active pile temperatures (2 °C during winter and 32 °C during summer).

Table 5. Thermo-mechanical properties of the materials.

Soil			
Mechanical Parameters		Thermal Parameters	
E_0 (MPa)	5.27	α_T (°C^{-1})	25. 10^{-6}
ν	0.3	λ (W.m/K)	1.25
E_c (MPa)	0.3	c_{Ts} (J/kg.K)	1700
ε_{vlimit}	Equ.(6)	c_{Tw} (J/kg.K)	4180 J/kg.K
		Initial porosity ϕ	0.52
		ρ_{cs} (kg/m^3)	2680
		ρ_{cw} (kg/m^3)	1000
Concrete Pile			
Mechanical Parameters		Thermal Parameters	
E (MPa)	20.10^3	α_T (°C^{-1})	1.2 10^{-5}
ν	0.26	λ (W.m/K)	0.8
		c_{Ts} (J/kg.K)	800

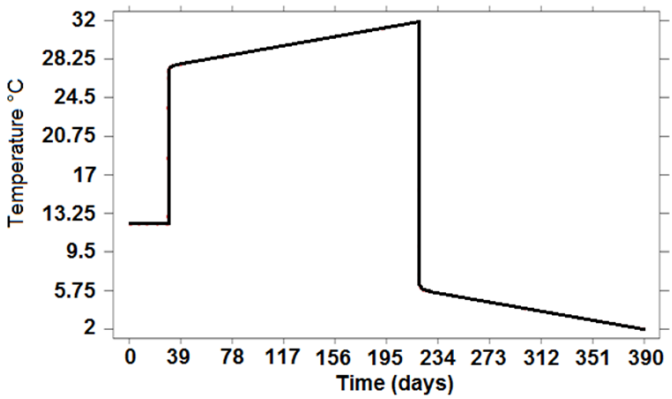

Figure 14. Thermal loading path.

The evolution of the ground temperature profile after the activation of the thermo-active pile was shown in Fig. 15. It can be observed that the ground temperature equilibrium is notably disturbed due to seasonal thermal variations in the pile. Furthermore, the ground temperature at a distance of approximately one pile diameter from the pile center changes completely over the entire depth of the pile length.

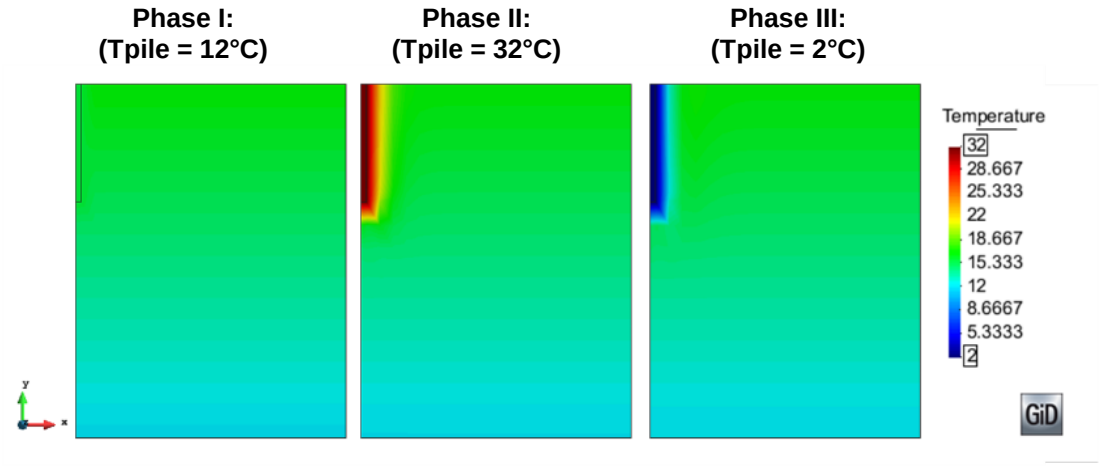

Figure 15. Temperature diffusion profiles at the end of each thermal loading.

The contour plot of temperature-induced axial displacement according to the diffusion within the system was shown in Fig. 16.The radial thermal displacements are insignificant compared to the axial thermal displacements due to the very small ratio between the diameter and the length of the pile. As expected, the extreme displacement values are concentrated within the concrete pile and at the soil surface. The negative values represent downward settlement, and the positive values represent upward heave.

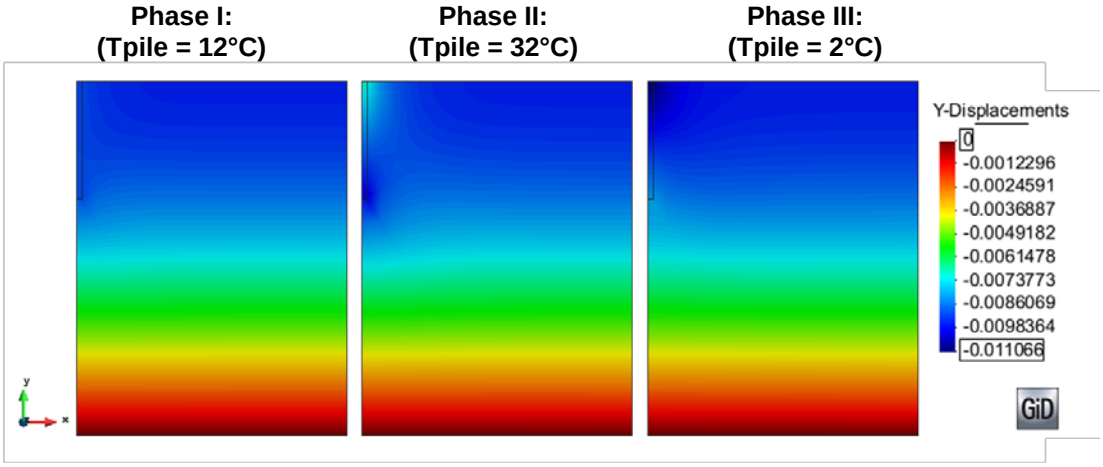

Figure 16. Contour of vertical displacement (in m) at the end of each thermal loading.

The effect of temperature variation on axial displacement at the soil surface was clearly visible in Fig. 17. During the first phase of loading, the settlement at the top of the pile corresponded to the response of the soil due to the applied mechanical load. In the progressive heating phase, the pile expanded with a relative head displacement of 2.1 mm. Then, the pile exhibited contractive behavior, and the final relative head displacement was –11 mm. However, over the entire length of the pile, there was a point that underwent no change in axial displacement over the entire period of thermal loading, called a null point as named by Knellwolf et al. [12], Bourne-Webb et al. [13].

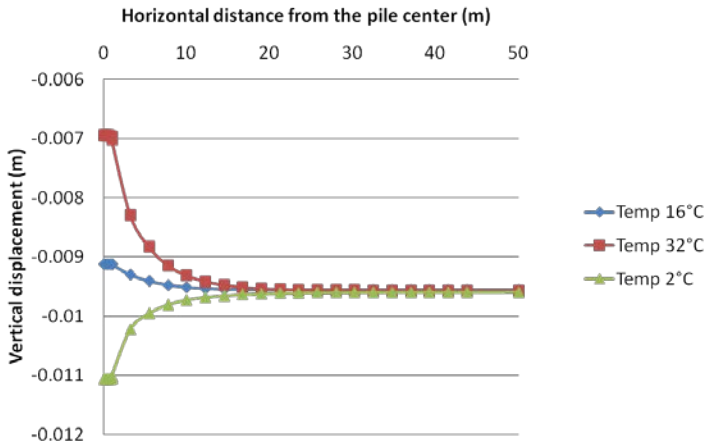

Figure 17. Vertical displacement at the soil surface at the end of each thermal loading step.

This point can be found in line with opposite responses to the movement of the head and of the base of the pile (Fig. 18). The latter is due to the lack of restraint at the pile head, which allows the pile to move freely. Thus, all the free thermal strain is observed. In Fig. 18 it can be observed that the null point moves with the imposed temperature. Therefore, the position of the null point depends not only on the pile confinement and the amount of freedom but also on the cyclic temperature variation.

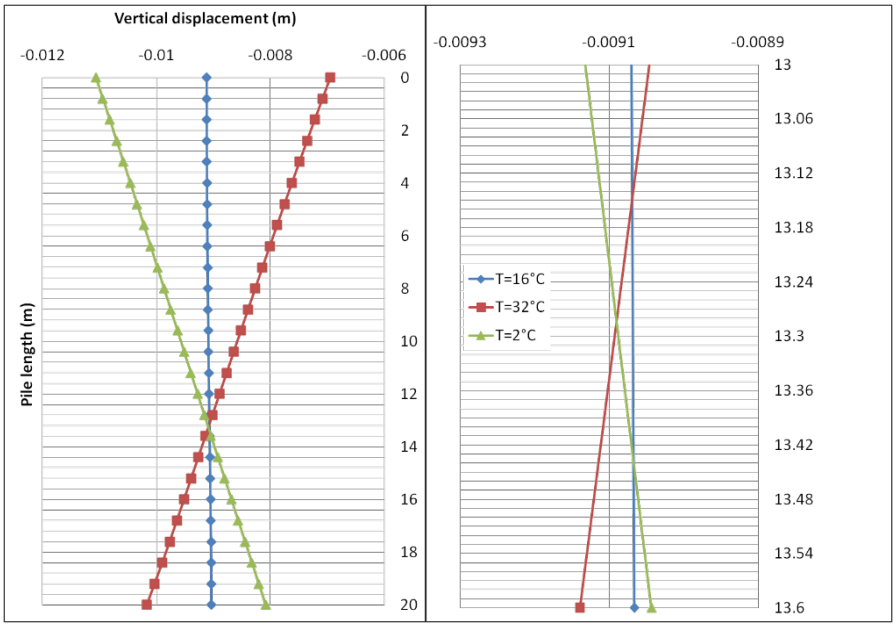

Figure 18. Mechanical response of the pile induced by temperature variation.

This model was used to investigate an alternative design method for a heat exchanger pile and the surrounding ground. The method developed depends on the pressuremeter parameters and their variation as functions of temperature. The case study was chosen to include the most representative characteristics of a heat exchanger pile, including seasonal temperature variations.

4. Conclusions

Experimental and numerical analysis of the effect of temperature on pressuremetric parameters have been conducted in this study. The main contributions of this paper include the followings:

1. The development and exploitation of an experimental device to study the effect of temperature on pressuremetric parameters;

2. The establishment of a simplified bilinear model with temperature-dependent parameters;

3. The development of a model problem of heat exchanger piles using this temperature-dependent bilinear model.

The results obtained with the mini-pressuremeter tests showed that the limit pressure and the creep pressure decrease with temperature while the pressuremeter modulus remains almost constant. These results reflect a softening behaviour with increasing temperature.

Next, a bilinear elastoplastic model was proposed to simulate the effect of temperature changes on mechanical parameters. To verify the proposed simplified model of the temperature-induced variations, a series of finite element simulations was developed that assumed controlled temperatures. Good agreement was reached between the experimental results and the model in which a relation between the parameters and temperature was proposed.

The proposed design method was finally used to study the coupled response of a heat exchanger pile. A case study was simulated using the newly developed approach. The results showed that the temperature variation inside the pile induced additional thermal stresses in the concrete pile and at the soil-pile contact zone. One novel aspect of the proposed thermo-mechanical model is that it takes into account the thermal dependency of the pressuremeter parameters.

References

1. Formentin, A., Pahud, D., Laloui, L., Moreni, M. Pieux échangeurs: conception et règles de prédimensionnement. Revue française de Génie Civil. 1999. 3 (6). Pp. 387–421. DOI: 10.1080/12795119.1999.9692263
2. Laloui, L., Moreni, M., Vulliet, L. Comportement d'un pieu bi-fonction. Canadian Geotechnical Journal. 2003. 40 (2). Pp. 388–402. DOI: 10.1139/t02-117

3. Brandl, H. Energy Foundations and other thermo-active ground structures: Géotechnique. 2006. 56 (2). Pp. 81–122. DOI: 10.1680/geot.2006.56.2.81
4. Péron, H., Knellwolf, C., Laloui, L. A Method for the Geotechnical Design of Heat Exchanger Piles. Geotechnical Special Publication. 2011. Pp. 470–479. DOI: 10.1061/41165(397)49
5. McCartney, J.S., LaHaise, D., LaHaise, T., Rosenberg, J.E. Application of Geoexchange Experience to Geothermal Foundations. Art of Foundation Engineering Practice. 2010. Pp. 411–422. DOI: 10.1061/41093(372)19
6. Modaressi, H., Laloui, L. A thermo-viscoplastic constitutive model for clays. International Journal for Numerical and Analytical Methods in Geomechanics. 1997. 21 (5). Pp. 313–335. DOI: 10.1002/(SICI)1096-9853(199705)21:5<313::AID-NAG872>3.0.CO;2-5
7. Burghignoli, A., Desideri, A., Milizaino, S. A laboratory study on the thermomechanical behavior of clayey soils. Canadian geotechnical journal. 2000. 37 (4). Pp. 764–780. DOI: 10.1139/cgj-37-4-764
8. Cekerevac, C., Laloui, L. Experimental study of thermal effects on the mechanical behaviour of a clay. International journal for numerical and analytical methods in geomechanics. 2004. 28 (3). Pp. 209–228. DOI: 10.1002/nag.332
9. Brandl, H. Energy piles and diaphragm walls for heat transfer from and into the ground. Proceedings of 3. International Seminar Deep Foundations on Bored and Auger Piles (BAP III), Ghent. 1998. Pp. 37–60. ISBN 90-5809-022-1
10. Bourne-Webb, P.J., Amatya, B., Soga, K., Amis, T., Davidson, C., Payne, P. Energy pile test at Lambeth College, London: geotechnical and thermodynamic aspects of pile response to heat cycles. Géotechnique. 2009. 59 (3). Pp. 237–248. DOI: 10.1680/geot.2009.59.3.237
11. Amatya, B.L., Soga, K., Bourne-Webb, P.J., Amis, T. and Laloui, L. Thermo-mechanical Behaviour of Energy Piles. Géotechnique. 2012. 62 (6). Pp. 503–519. DOI: 10.1680/geot.10.P.116
12. Knellwolf, C., Péron, H., Laloui, L. Geotechnical Analysis of Heat Exchanger Piles. Journal of Geotechnical and Geoenvironmental Engineering. 2011. 137(10). Pp. 890–902. DOI: 10.1061/(ASCE)GT.1943-5606.0000513
13. Bourne-Webb, P.J., Amatya, B.L., Soga, K. A framework for understanding energy pile behaviour. Proceedings of the Institution of Civil Engineers – Geotechnical Engineering. 2013. 166 (2). Pp. 170–177. DOI: 10.1680/geng.10.00098
14. Graham, J., Tanaka, N., Crilly, T., Alfaro, M. Modified Cam-Clay modeling of temperature effects in clays. Canadian Geotechnical Journal. 2001. 38 (3). Pp. 608–621. DOI: 10.1139/cgj-38-3-608
15. Goodman, R.E., Taylor, R.L. Brekke, T.L. A model for the mechanics of jointed rock. Journal of the Soil Mechanics and Foundations Divisions. 1968. 94 (3). Pp. 637–659.
16. De Gennaro, V., Frank, R. Modélisation de l'interaction sol-pieu par la méthode des éléments finis. In Bulletin des Laboratoires des Ponts et Chaussées: 256–257. Paris, 2005. Pp. 107–133.
17. Said, I. Comportement des interfaces et modélisation des pieux sous charge axiale. Sciences of the Universe. Ecole des Ponts Paris Tech, 2006. 274 p.
18. Desai, C., Faruque, M. Constitutive model for (geological) materials. Journal of Engineering Mechanics. 1984. 110(9). Pp. 1391–1408.
19. Randolph, M.F. Worth, C.P. Analysis of deformation of vertically loaded piles. Journal of Geotechnical Engineering Division. 1978. 104 (12). Pp. 1465–1488.
20. Frank, R., Zhao, S.R. Estimation par les paramètres pressiométriques de l'enfoncement sous charge axiale des pieux forés dans les sols fins. Bull. liaison Labo P. et Ch., 119 Paris. 1982. Pp. 17–24.
21. Armaleh, S., Desai, C.S. Load-deformation response of axially loaded piles. Journal of Geotechnical Engineering. 1987. 113 (12). Pp. 1483–1500.
22. AFNOR, NF P94-110-1. Sols: reconnaissance et essais; Essai pressiométrique Ménard – Partie 1: essai sans cycle. Paris: Association Française de Normalisation. 2000.
23. ASTM, D 4719–07. Standard Test Methods for Prebored Pressuremeter Testing in Soils. West Conshohocken: ASTM International (Unified Soil Classification System). 2007.
24. Olgun, C.G., Ozudogru, T.Y., Arson, C.F. Thermo-mechanical radial expansion of heat exchanger piles and possible effects on contact pressures at pile-soil interface. Géotechnique Letters. 4 (3). 2014. Pp. 170–178. DOI: 10.1680/geolett.14.00018
25. Abuel-Naga, H.M., Bergado, D.T. Chaiprakaikeow, S. Innovative thermal technique for enhancing the performance of prefabricated vertical drain during the preloading process. Geotextiles and Geomembranes. 2006. 24 (6). Pp: 359–370. DOI: 10.1016/j.geotexmem.2006.04.003
26. Abuel-Naga, H.M., Bergado, D.T., Bouazza, A. Ramana, G.V. Volume change behavior of saturated clays under drained heating conditions: experimental results and constitutive modeling. Canadian Geotechnical Journal. 2007. 44 (8). Pp. 942–956. DOI: 10.1139/t07-031
27. Shoukry, S.N., William, G.W., Downie, B., Riad, M.Y. Effect of moisture and temperature on the mechanical properties of concrete. Construction and Building Materials. 2011. 25 (2). Pp. 688–696. DOI: 10.1016/j.conbuildmat.2010.07.020
28. Abuel-Naga, H.M., Bergado, D.T., Grino, L., Rujivipat, P. Thet, Y. Experimental evaluation of engineering behavior of soft bangkok clay under elevated temperature. Journal of Geotechnical and Geoenvironmental Engineering. 2006. 132 (7). Pp. 902–910. DOI: 10.1061/(ASCE)1090-0241(2006)132:7(902)
29. Abuel-Naga, H.M., Bergado, D.T., Lim, B.F. Effect of temperature on shear strength and yielding behavior of soft Bangkok clay. Soils and Foundations. 2007. 47 (3). Pp. 423–436. DOI: 10.3208/sandf.47.423
30. Abuel-Naga, H.M., Bergado. D.T., Bouazza, A. Pender, M.J. Thermomechanical model for saturated clays. Geotechnique. 2009. 59(3). Pp. 273–278. DOI: 10.1680/geot.2009.59.3.273
31. GSHPA. Thermal Pile Design, Installation and Materials Standards, Ground Source Heat Pump Association, [Online]. System requirements: Adobe Acrobat Reader. URL: http://www.gshp.org.uk/GSHPA_Thermal_Pile_Standard.html. (date of application: 07.10.2021).
32. Turner, M.J., Clough, R.W., Martin, H., Topp, J. Stiffness and deflection analysis of complex structures. Journal of the Aerospace Sciences. 1956. 23 (9).
33. Tanaka, N., Graham, J. Crilly, T. Stress-strain behaviour of reconstituted illitic clay at different temperatures. Engineering Geology. 1997. 47 (4). Pp. 339–350. DOI: 10.1016/S0013-7952(96)00113-5

34. Lynch, F.L. Frio shale mineralogy and the stoichiometry of the smectite-to-illite reaction: the most important reaction in clastic sedimentary diagenesis. Clays and Clay Minerals. 1997. 45 (5). Pp. 618–631.
35. AFNOR, NF P94-051. Sols: reconnaissance et essais - Détermination des limites d'Atter-berg – Limite de liquidité à la coupelle – Limite de plasticité au rouleau. Paris: Association Française de Normalisation. 1993.
36. GTR. Guide technique: Réalisation des remblais et des couches de forme. Paris: LCPC. 2000.
37. ASTM, D 2487–06. Standard Practice for Classification of Soils for Engineering Purposes. West Conshohocken: ASTM International (Unified Soil Classification System). 2006.
38. Lingnau, B.E., Graham, J., Yarechewski, D., Tanaka, N., Gray, M.N. Effects of temperature on strength and compressibility of sand-bentonite buffer. Engineering Geology. 1996. 41(1-4). Pp. 103–115. DOI: 10.1016/0013-7952(95)00028-3
39. Leroueil, S., Marques, M.E.S., Almeida, M.S.S. Viscous behaviour of St-Roch-de-l'Achigan clay, Quebec. Canadian Geotechnical Journal. 2004. 41 (1). Pp. 25–38. DOI: 10.1139/t03-068
40. Uchaipichat, A., Khalili, N. Experimental investigation of thermo-hydro-mechanical behaviour of an unsaturated silt. Géotechnique. 2009. 59 (4). Pp. 339–353. DOI: 10.1680/geot.2009.59.4.339
41. Olivella, S., Gens, A., Ramirez, J. C., Alonso, E.E. Numerical formulation for a simulator (Code_Bright) for the coupled analysis of saline media. Engineering Computations. 1996. 13 (7). Pp. 87–112. DOI: 10.1108/02644409610151575
42. DeVries, D.A. Afgan, N.H. Heat and Mass Transfer in the Biosphere. Scripta book Co. Washington. 1975.
43. Brandon, T.L., Mitchell, J.K. Factors influencing the thermal resistivity of sands. Journal of the Geotechnical Engineering. 1989. 115 (12). Pp. 1683–1698.
44. Mitchell, J.K. Fundamental of soil behavior. John Wiley &Sons, Inc. New York. 1993.
45. Ménard, L. The Ménard Pressuremeter: Interpretation and Application of Pressuremeter Test Results to Foundation Design, Sols-Soils. 1975. 26 p.
46. Hueckel, T., Borsetto, M. Thermoplasticity of saturated soils and shales: constitutive equations. Journal of Geotechnical Engineering. 1990. 116 (12). Pp. 1765–1777. DOI: 10.1061/(ASCE)0733-9410(1990)116:12(1765)
47. Laloui, L. Thermo-mechanical behavior of soils. Revue Française de Génie Civil. 2001. 5 (6). Pp. 809–843. DOI: 10.1080/12795119.2001.9692328
48. Suryatriyastuti, M.E., Mroueh, H., Burlon, S. Understanding the temperature-induced mechanical behaviour of energy pile foundations. Renewable and Sustainable Energy Reviews. 2012. 16 (5). Pp. 3344–3354. DOI: 10.1016/j.rser.2012.02.062

Information about authors:

Wahib Arairo, *PhD*
ORCID: https://orcid.org/0000-0002-1708-0233
E-mail: wahib.arairo@balamand.edu.lb

Farimah Masrouri, *PhD*
ORCID: https://orcid.org/0000-0001-6680-494X
E-mail: Farimah.Masrouri@ensg.inpl-nancy.fr

Adel Abdallah, *PhD*
ORCID: https://orcid.org/0000-0001-9784-2818
E-mail: adel.abdallah@univ-lorraine.fr

Sandrine Rosin-Paumier, *PhD*
ORCID: https://orcid.org/0000-0001-9271-7153
E-mail: sandrine.rosin@univ-lorraine.fr

Omar Sraj,
ORCID: https://orcid.org/0000-0002-7163-9915
E-mail: omar.sraj@hotmail.com

Milad Khatib, *PhD*
ORCID: https://orcid.org/0000-0002-0140-0941
E-mail: milad.khatib@isae.edu.lb

Received 22.09.2021. Approved after reviewing 23.06.2022. Accepted 27.06.2022.